Cell Transplantation, Vol. 17, pp. 679–694, 2008
Printed in the USA.

0963-6897/08 $90.00 + .00
E-ISSN 1555-3892
www.cognizantcommunication.com

Different Cardiovascular Potential of Adult- and Fetal-Type Mesenchymal Stem Cells in a Rat Model of Heart Cryoinjury

Laura Iop,* Angela Chiavegato,* Andrea Callegari,* Sveva Bollini,† Martina Piccoli,† Michela Pozzobon,† Carlo Alberto Rossi,† Sara Calamelli,* David Chiavegato,* Gino Gerosa,‡ Paolo De Coppi,†§ and Saverio Sartore*

*Department of Biomedical Sciences, University of Padua School of Medicine, Padua, Italy
†Department of Pediatrics, University of Padua School of Medicine, Padua, Italy
‡Department of Cardiologic, Thoracic and Vascular Sciences, University of Padua School of Medicine, Padua, Italy
§Surgery Unit, Great Ormond Street Hospital and Institute of Child Health, University College London, London, UK

Efficacy of adult (bone marrow, BM) versus fetal (amniotic fluid, AF) mesenchymal stem cells (MSCs) to replenish damaged rat heart tissues with new cardiovascular cells has not yet been established. We investigated on the differentiation potential of these two rat MSC populations in vitro and in a model of acute necrotizing injury (ANI) induced by cryoinjury. Isolated BM-MSCs and AF-MSCs were characterized by flow cytometry and cytocentrifugation and their potential for osteogenic, adipogenic, and cardiovascular differentiation assayed in vitro using specific induction media. The left anterior ventricular wall of syngeneic Fisher 344 ($n = 48$) and athymic nude (rNu) rats ($n = 6$) was subjected to a limited, nontransmural epicardial ANI in the approximately one third of wall thickness without significant hemodynamic effects. The time window for in situ stem cell transplantation was established at day 7 postinjury. Fluorochrome (CMTMR)-labeled BM-MSCs (2×10^6) or AF-MSCs (2×10^6) were injected in syngeneic animals ($n = 26$) around the myocardial lesion via echocardiographic guidance. Reliability of CMTMR cell tracking in this context was ascertained by transplanting genetically labeled BM-MSCs or AF-MSCs, expressing the green fluorescent protein (GFP), in rNu rats with ANI. Comparison between the two methods of cell tracking 30 days after cell transplantation gave slightly different values (1420,58 ± 129,65 cells/mm^2 for CMTMR labeling and 1613.18 ± 643.84 cells/mm^2 for genetic labeling; p = NS). One day after transplantation about one half CMTMR-labeled AF-MSCs engrafted to the injured heart (778.61 ± 156.28 cells/mm^2) in comparison with BM-MSCs (1434.50 ± 173.80 cells/mm^2, $p < 0.01$). Conversely, 30 days after cell transplantation survived MSCs were similar: 1275.26 ± 74.51/mm^2 (AF-MSCs) versus 1420.58 ± 129.65/mm^2 for BM-MSCs (p = NS). Apparent survival gain of AF-MSCs between the two time periods was motivated by the cell proliferation rate calculated at day 30, which was lower for BM-MSCs (6.79 ± 0.48) than AF-MSCs (10.83 ± 3.50; $p < 0.01$), in the face of a similar apoptotic index (4.68 ± 0.20 for BM-MSCs and 4.16 ± 0.58 for AF-MSCs; p = NS). These cells were also studied for their expression of markers specific for endothelial cells (ECs), smooth muscle cells (SMCs), and cardiomyocytes (CMs) using von Willebrand factor (vWf), smooth muscle (SM) α-actin, and cardiac troponin T, respectively. Grafted BM-MSCs or AF-MSCs were found as single cell/small cell clusters or incorporated in the wall of microvessels. A larger number of ECs (227.27 ± 18.91 vs. 150.36 ± 24.08 cells/mm^2, $p < 0.01$) and CMs (417.91 ± 100.95 vs. 237.43 ± 79.99 cells/mm^2, $p < 0.01$) originated from AF-MSCs than from BM-MSCs. Almost no SMCs were seen with AF-MSCs, in comparison to BM-MSCs (98.03 ± 40.84 cells/mm^2), in concordance with lacking of arterioles, which, instead, were well expressed with BM-MSCs (71.30 ± 55.66 blood vessels/mm^2). The number of structurally organized capillaries was slightly different with the two MSCs (122.49 ± 17.37/mm^2 for AF-MSCs vs. 148.69 ± 54.41/mm^2 for BM-MSCs; p = NS). Collectively, these results suggest that, in the presence of the same postinjury microenvironment, the two MSC populations from different sources are able to activate distinct differentiation programs that potentially can bring about a myocardial–capillary or myocardial–capillary–arteriole reconstitution.

Key words: Cardiac injury; Experimental model; Stem cells; Cardiac cell regeneration; Fetal stem cells; Adult stem cells

Received November 16, 2006; final acceptance September 19, 2007.
Address correspondence to Saverio Sartore, Ph.D., Department of Biomedical Sciences, University of Padua, Viale G. Colombo, 3, 35121 Padua, Italy. Tel: +390498276481; Fax: +390498276040; E-mail: saverio.sartore@unipd.it

INTRODUCTION

A dramatic hurdle to cardiac wound healing in rats and other mammals is represented by the low regenerating capacity of the myocardium in the face of the high regenerative ability of vascular endothelial cells (ECs) and smooth muscle cells (SMCs) (14). These properties in combination with scar tissue formation and low blood supply, as a result of the postinjury inflammatory response, produce a left ventricular dysfunction, possibly culminating in heart failure (21). In principle, replacement of damaged vascular tissue and myocardium with new cardiovascular units should restore the contractile function or, at least, regain part of the original structural and functional properties (23). Cardiovascular cell replenishment after acute myocardial infarction (AMI), or reduction/slowing down of progressive functional deterioration in the case of prolonged ischemia, are to be addressed by two different strategies: 1) implementation of angiogenesis and arteriogenesis along with cardiogenesis (via local activation or extracardiac mobilization of cell precursors, or exogenous administration of committed or precursor cells) (1,15,19), or 2) inducing angiogenesis/arteriogenesis followed by cardiogenesis if the local conditions can permit this sequential cell colonization (11).

To this end, the choice of stem cell type to be used in therapeutic cardiovascular regeneration of acute or chronic myocardial ischemia could be of paramount importance if specific combinations of differentiated cell phenotypes are to be obtained. Hence, which stem cell is most suitable for transplantation in the injured heart? Conceptually, the "immature" (embryonic, fetal, or early postnatal) stem cells (42) seem to possess the ability to deal with this "multilineage task" (5), but their efficacy is still questionable, especially for their capacity to increase electric instability in the heart (49) and because of their immunostimulatory potential (37). On the other hand, adult-type bone marrow (BM)-derived mesenchymal stem cells (MSCs) differentiate into, besides other cell lineages, ECs, SMCs, and cardiomyocytes (CMs) but their availability is limited and their preparation requires an invasive procedure (41). In the context of "immature" stem cells, the use of fetal stem cells from extra-embryonic tissues may circumvent many of ethical concerns related to use of embryonic ones. Indeed, human placenta (47), amnion (28), amniotic fluid (AF)-derived (7,17,20,39), umbilical cord perivascular vein (2), or blood (16,30) adherent MSCs display some properties relevant to a clinical application such as multipotency and a low immunogenicity [at least for placenta-derived MSCs (24)] (3). Our recent results on the effect of BM-MSCs and AF-MSCs when transplanted in the rat injured bladder suggest that these cells have a limited differentiation potential but they can regulate the postinjury remodeling (i.e., preventing compensatory hypertrophy of survived SMCs) (8).

Our goal in this comparative study is to ascertain capability of surviving and cardiovascular cell potential of BM-MSCs versus AF-MSCs using a rat syngeneic model of cardiac nontransmural acute necrotizing injury (ANI).

MATERIALS AND METHODS

Animals and ANI Model

Experiments were performed with 48 male Fisher 344 rats (Charles River, Milan Italy) weighing 220–250 g and six athymic nude rats weighing 200–220 g (rNu; Charles River) (Table 1). The investigation conformed to the Guide for Care and Use of Laboratory Animals prepared by the Institute of Laboratory Animal Resources, National Research Council, published by the National Academy Press, revised 1996 (NIH Publication No. 85-23) and the Italian Health Minister Guidelines for Animal Research. The protocol was approved by the University of Padua Animal Care Committee. The animals were anesthetized by tiletamine hydrochloride-zolazepam (IM; 9 mg/100 g body weight; Zoletil; Virbac, Carros, France) along with xylazin (SC; 0.4 mg/100 g; Xilor; Bio 98, s.r.l., Bologna, Italy), and atropine (IP; 5 μg/100 g; VaxServe, Scranton, PA), intubated, and mechanically ventilated (Harvard, South Natick, MA) with room air. The heart was exposed through a left thoracotomy (third or four intercostal space) and an ANI (freeze–thaw procedure) was created by two sequential exposures (15 s each, 30 s of nonfreezing interval) of a liquid nitrogen-cooled cryoprobe (a stainless steel cylinder, 5 mm of diameter). ANI was localized at about 3 mm from the apex, in the left ventricular anterior wall. ANI was confirmed by wall blanching followed by hyperemia. The chest was then closed and the animals weaned from the respirator, extubated, and treated with antibiotics (20 mg/100 g; Baytril, Bayer, Milan, Italy). A group of Fisher rats ($n = 10$; Group 1, Table 1) was sacrificed at different intervals from ANI induction for histological and immunohistochemical evaluation of the best time window for intramyocardial MSC transplantation.

Cell Preparation

BM-MSCs were obtained from femurs and tibias of 4-week-old male Fisher 344 or transgenic GFP-expressing rats (kindly provided by Dr. Masaru Okabe, Genetical Research Information Center, Osaka University, Osaka, Japan). Cells were resuspended in MEMα (Sigma, St. Louis, MO) supplemented with 20% FBS (Invitrogen, Carlsbad, CA), 1% streptomycin and penicillin solution (Sigma). AF-MSCs were prepared from the

Table 1. Animal Groups Used in This Study

	Days After ANI Induction				
	Day 1	Day 7	Day 15	Day 21	Day 30
Group 1: ANI rats (for the study of lesion development)	$n = 2$	$n = 2$	$n = 2$	$n = 2$	$n = 2$
	Days After Transplantation				
	Day 1	Day 10	Day 30		
Group 2: ANI rats (for open-chest practice of cell delivery)	$n = 6$*	—	—		
Group 3: ANI rats (Fisher) + CMTMR-BM-MSCs	$n = 3$	$n = 5$	$n = 5$		
Group 4: ANI rats (Fisher) + CMTMR-AF-MSCs	$n = 3$	$n = 5$	$n = 5$		
Group 5: ANI rats (rNu) + GFP-BM-MSCs	—	—	$n = 3$		
Group 6: ANI rats (rNu) + GFP-AF-MSCs	—	—	$n = 3$		
Group 7: ANI rats (Fisher) + medium	$n = 2$	$n = 2$	$n = 2$		

ANI, acute necrotizing injury; BM-MSCs, bone marrow mesenchymal stem cells; AF-MSCs, amniotic fluid mesenchymal stem cells; CMTMR, 5-(and 6)-4-chloromethyl (benzoyl)amino-tetramethylrhodamine; GFP, green fluorescent protein; rNu, nude, athymic rats.
*Three rats were sacrificed immediately after dye injection and three were killed 24 h after cell injection (see Materials and Methods).

AF of a pregnant rat of Fisher or GFP-expressing strain at 16 days postcoitum. AF was picked up by a microsyringe under magnification lens and resuspended in Amniotic Culture Medium (ACM) [63% MEMα (Sigma), 20% Chang medium C (Irvine Scientific, Santa Ana, CA), 15% FBS, 1% streptomycin-penicillin solution, and 1% L-glutamine]. Cell seeding was performed at a density of 5000 cells/cm^2 on non-tissue culture petri dishes (BD Falcon™, BD Biosciences). After 7 days, nonadherent cells and debris were discarded and the adherent cells cultivated until preconfluency. Adherent cells were detached from the plastic plate using a trypsin-sodium-EDTA solution (Sigma) and then repeatedly passaged. Cell morphology was studied using a phase contrast Leica DM IRB microscope (Leica, Wetzlar, Germany) connected with a Canon Power Shot S40 camera.

Flow Cytometry and Cytocentrifugation

Flow cytometric analysis was performed at the second and third passage. BM-MSCs and AF-MSCs were detached by adding citrate buffer (Sigma), rinsed, and resuspended in PBS at a concentration of 5×10^5 cells/100 μl. Cells were stained directly with 10 μl of FITC fluorochrome-labeled anti-rat CD90 (BD-Biosciences, San Diego, CA), CD44 (BD-Biosciences), PE-conjugated anti-rat antibodies to the progenitor markers CD45 (BD-Biosciences), CD73 (BD-Biosciences), and MHC-II (BD-Biosciences). Cytometric analysis was performed using a COULTER Epics XL-MCL cytometer (Beckman Coulter), and data were elaborated by means of EXPO™ 32 ADC Software.

Cytospin preparations of BM-MSCs and AF-MSCs were obtained with a Shandon Cytospin 4 centrifuge (Thermo Fisher Scientific, Inc., Waltham, MA). Cytospin-obtained cells were fixed in 2% *p*-formaldehyde in PBS, pH 7.2, and then incubated with the primary antibody to cytoplasmic antigens of the cardiogenic and noncardiogenic cell lineages as well as embryonic antigens for 30 min at 37°C. The primary antibodies used in the immunofluorescence experiments were the following: anti-SSEA4 (Chemicon, Temecula, CA); anti-Oct-4 (Santa Cruz, Santa Cruz, CA); anti-CD117 (Santa Cruz); anti-CD271 (BD-Biosciences), anti-CD105 (Cymbus, Chandlers Ford, UK); anti-Flk-1 (Santa Cruz); anti-von Willebrand factor (vWf) (Dako, Dakopatts, Denmark); anti-smooth muscle (SM) α-actin (Sigma); anti-SM22 (Abcam, Cambridge, UK); anti-vimentin (Dako); anti-pan-cytokeratin (Sigma). The secondary antibodies were the Cy2-conjugated goat Fab′ to mouse or rabbit IgGs (Chemicon). Manual counting of cytocentrifuged cells positive with each antibody was performed by two independent examiners and the corresponding scores, expressed as percentage of total Hoechst-stained, cells, distributed in five classes (see also legend to Table 2). Flow cytometry and cytocentrifugation analysis were performed in triplicate using distinct MSC preparations.

In Vitro Phenotypic Profiling of BM-MSCs and AF-MSCs

In vitro potential for osteogenic and adipogenic differentiation as well as stability of antigenic marker expression and propensity to cell phenotypic conversion

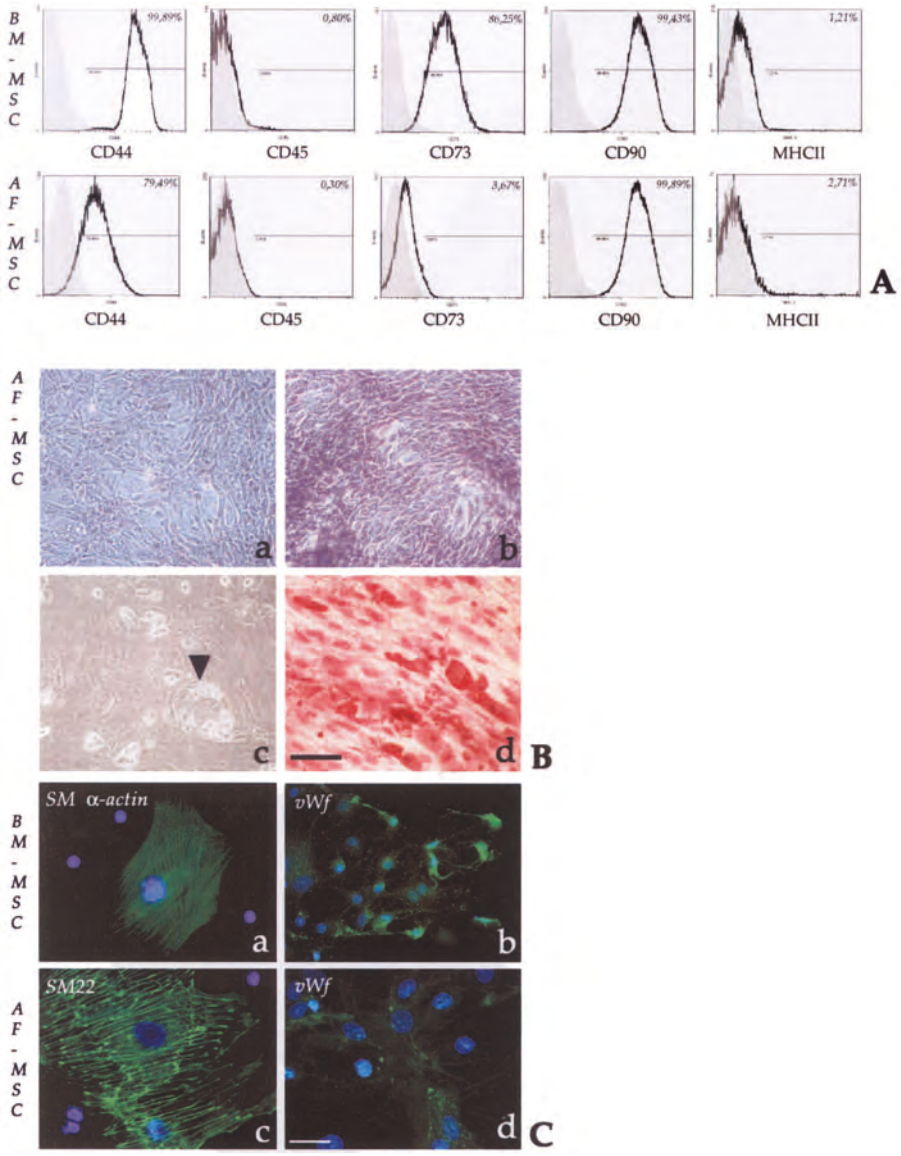

Figure 1. Flow cytometry pattern (A), osteogenic and adipogenic (B), and vascular (C) differentiation potential of BM-MSCs and AF-MSCs. Note the different profile of the two MSCs with CD73. (B) Control (a) and AP-positive reaction (b) after exposure of AF-MSCs to osteogenic medium; (c, d) phase contrast and Oil-Red-O staining, respectively, of a AF-MSC culture treated with the adipogenic medium. The black arrowhead in (c) shows a cell cluster filled with fat droplets. Scale bar: 80 μm. (C) Immunofluorescence patterns of cultured BM-MSCs (a, b) and AF-MSCs (c, d) grown in differentiation media specific for SMCs (a, c) or ECs (b, d). Scale bar: 50 μm.

for cardiovascular cell lineages were evaluated for BM-MSCs and AF-MSCs. All experiments were performed using cells passaged up to the third passage and then incubated in specific differentiation media or cocultured with neonatal CMs.

Osteogenic Differentiation

Cells were seeded at 2000 cells/cm^2 in 35-mm plates (Falcon, BD) and cultured in DMEM low-glucose medium (Sigma) with 10% FBS (Invitrogen), 1% penicillin/streptomycin (Invitrogen), and osteogenic supplements (100 nM dexamethasone, 10 mM β-glycerophosphate, and 0.05 mM ascorbic acid-2-phosphate (Sigma-Aldrich)). Osteogenic condition was maintained for a week with medium changes three times per week. Osteogenesis was assessed at day 7. Alkaline phosphatase (AP) activity of these cultures was determined according to the manufacturer's instructions (Sigma-Aldrich). Briefly,

Table 2. Immunophenotyping of Rat BM-MSCs and AF-MSCs as Determined by Cytospin Analysis (Before Transplantation)

Antigen	BM-MSCs	AF-MSCs
SSEA4	+/– (8%)	+ (15%)
Oct-4	+/– (4%)	++ (34%)
vWf	+ (14%)	+ (10%)
Flk-1	+/– (7%)	+ (12%)
CD117	–	–
CD271 (NGF-R)	+ (16%)	++ (35%)
CD105 (endoglin)	++ (40%)	+++ (81%)
SM α-actin	+ (15%)	+/– (5%)
SM22	+ (17%)	+/– (6%)
Vimentin	++++ (90%)	++++ (95%)
Pan-cytokeratin	–	–

–: no positive cells; +/–: <10%; +: 10–30%; ++: 30–60%; +++: 60–90%; ++++: >90%.

cells were fixed in acetone for 30 s. Substrate (fast blue RR solution with naphthol AS-MX alkaline phosphate solution) was added to the cells in culture dishes; nuclei were counterstained with Mayer's hematoxylin.

Adipogenic Differentiation

Cells were treated with adipogenic medium for 3 weeks. The medium was changed three times a week, and adipogenesis was assayed at days 7 and 21. Adipogenic medium was as follows: low-glucose DMEM supplemented with 10% FBS, 1% antibiotics, and adipogenic supplements [1 mM dexamethasone, 1 mM 3-isobutyl-1-methylxanthine, 10 μg/ml insulin, 60 mM indomethacin (Sigma-Aldrich)]. Fat vesicles accumulated in these cell cultures were determined by Oil-Red-O staining (Sigma). After fixation in 10% formalin, cells were incubated with Oil-Red-O staining solution and then counterstained with Mayer's hematoxylin.

Cardiovascular Differentiation

Cells were seeded at 1×10^4 cells/cm^2 and induction of SMC or EC differentiation in both types of MSCs was achieved by growing cells in DMEM with 10% FBS, 5% horse serum (HS) (Invitrogen), and 50 μM hydrocortisone (Sigma) (50) or endothelial cell growth medium (Promo Cell, Heidelberg, Germany), respectively. Induction of CM differentiation in MSCs was carried out according to Shim et al. (33) using DMEM containing 10% FBS for 3 days. Before confluency, MSCs were shifted to Cardiac Differentiation Medium and grown for 15 days.

Neonatal CM were obtained by trypsin-EDTA digestion from newborn rat hearts resuspended in culture plating medium (CPM) [68% DMEM (Invitrogen), 17% M-199 (Sigma), 5% FBS (Invitrogen), 10% HS (Invitrogen)].

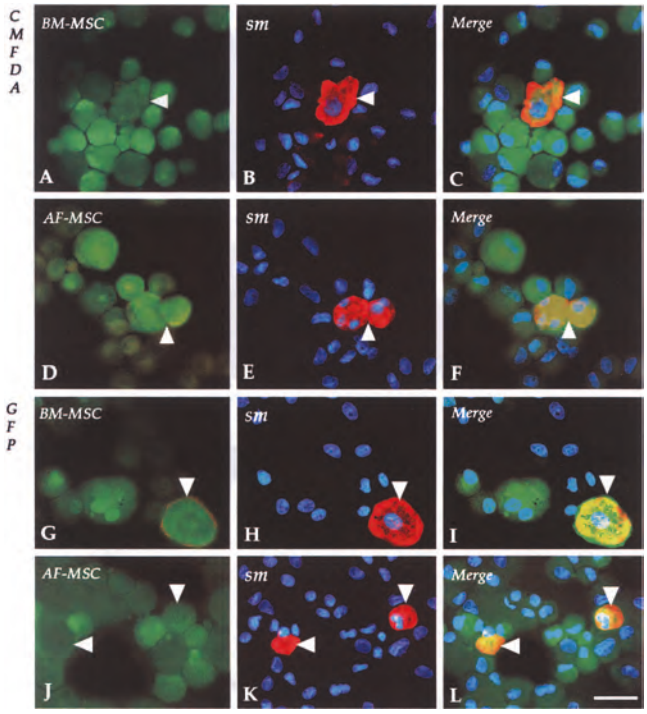

Figure 2. Immunofluorescence patterns of BM-MSCs and AF-MSCs labeled with CMFDA (A–F) or GFP (G–L) cocultured with neonatal CM. Green fluorochromes are shown in (A, D, G, J); sarcomeric myosin (*sm*) binding is in red (B, E, H, K). White arrowheads indicate rare MSCs expressing sarcomeric myosin; some of them appear multinucleated. Scale bar: 50 μm.

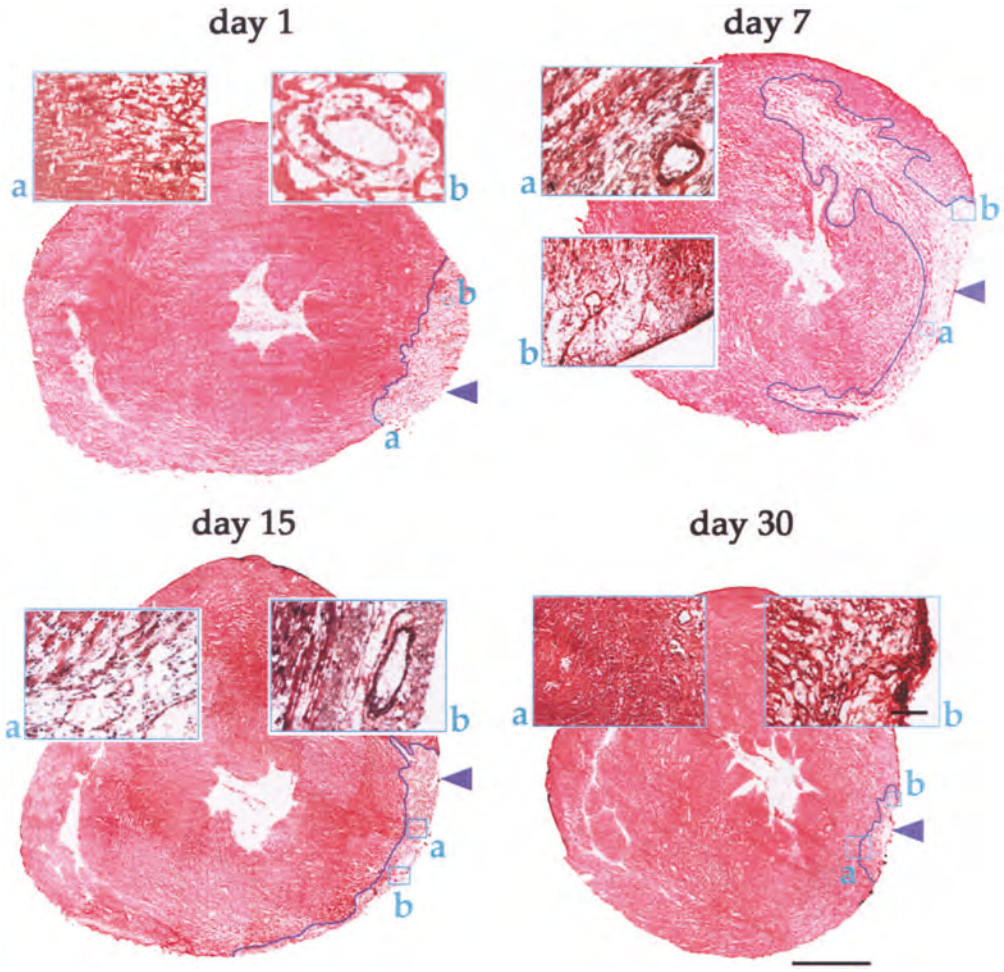

Figure 3. H&E staining of equatorial cardiac cryosections taken at 1, 7, 15, and 30 days after cryoinjury. Specific magnifications of some areas pertaining to each cryosection are boxed and identified by letters (a, b). Note the progressive reduction of ANI size with time and the scarring of lesion at day 30. Scale bar: 80 μm (in the boxes); 1 cm (whole cryosections).

Conditioned media from cultures of neonatal CM ("beating cell cultures") were also collected and applied to MSCs up to day 10 of cultivation.

Cocultures of BM-MSCs or AF-MSCs (from Fisher or GFP strain) with rat neonatal CM (Fisher) were established as follows. Each MSC type was mixed in the ratio 1:4 with freshly prepared CM and seeded at a density of 8×10^3 cells/cm^2. MSCs obtained from the Fisher strain had been previously labeled with 10 μM cell tracker chloromethylfluorescein diacetate (CMFDA) following the instructions of the manufacturer (Molecular Probes, Eugene, OR) whereas GFP-MSCs were used as such. Cell viability after cell labeling was monitored by trypan blue exclusion test. After 9 days of cocultures in CPM, cells were fixed in 2% *p*-formaldehyde (Sigma) in PBS, pH 7.2. Alternatively, cells were then rapidly detached with trypsin-EDTA and cytocentrifuged at 550 rpm. Cocultures were carried out in triplicate.

Antibody Labeling

Cover slips and cytospins with MSCs grown in the differentiating or conditioned media or in cocultures were fixed in 2% *p*-formaldehyde in PBS and tested in single or double immunofluorescence using anti-vWf (Dako); anti-SM α-actin (Sigma); anti-SM22 (Abcam); anti-cardiac troponin T (cTnT; Abcam); MF-20 anti-sarcomeric myosin (*sm*; Hybridoma Bank, Iowa City, IA) as primary antibodies and Cy2-conjugated goat Fab′ to mouse or rabbit IgGs (Chemicon) as secondary antibodies. In coculture experiments, GFP was enhanced by a rabbit anti-GFP antibody (Molecular Probes) and revealed by a Cy2-conjugated goat Fab′ to rabbit IgG (Chemicon), while cTnT and sm were labeled with a Alexa Fluor 594-conjugated goat Fab′ to mouse IgG (Molecular Probes). Distribution of antigens was studied using a Zeiss Axioplan epifluorescence microscope

(Zeiss, Oberkochen, Germany), and images were acquired using a Leica DC300F digital videocamera (Leica, Wetzlar, Germany). Cells grown in coculture conditions showing sm expression were counted as a percentage of CMFDA-labeled or GFP-expressing MSCs.

Echocardiography

Transthoracic echocardiograms were obtained from sham-operated and operated animals (7 and 30 days after ANI). Rats were kept in lateral decubitus position after being anesthetized with xylazine (0.16 mg/100 g) and tiletamine-zolazepam (4.5 mg/100 g). A Sonos 5500 echocardiographic system (Philips Hewlett-Packard, Palo Alto, CA) equipped with a 12.5-MHz transducer was placed on the hemithorax. A two-dimensional short-axis view of left ventricle (LV) was initially used at the level of papillary muscles to obtain targeted M-mode tracings that were recorded on videotape. This orientation allowed for delineation of wall thickness and motion in ANI and non-ANI regions. A veterinarian and a physician who where unaware of rat treatment analyzed the images. Data were elaborated to calculate the fractional shortening, ejection fraction, wall thickness, and ventricular volume for each animal (34). Variability in the echocardiographic measurements obtained by the two examiners was less than 5% (both inter- and intraobserver values).

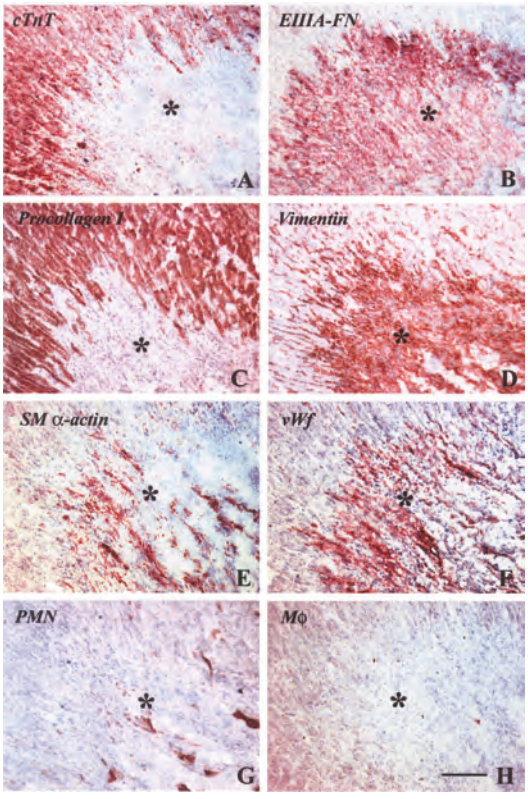

Figure 4. Immunohistochemical staining of the cryoinjured region (7 days after injury) with antibodies to cTnT (A), EIIIA-FN (B), procollagen I (C), vimentin (D), SM α-actin (E), vWf (F), PMN (G), and Mϕ; (H). The cardiac scarring area is indicated by the asterisk. Scale bar: 100 μm.

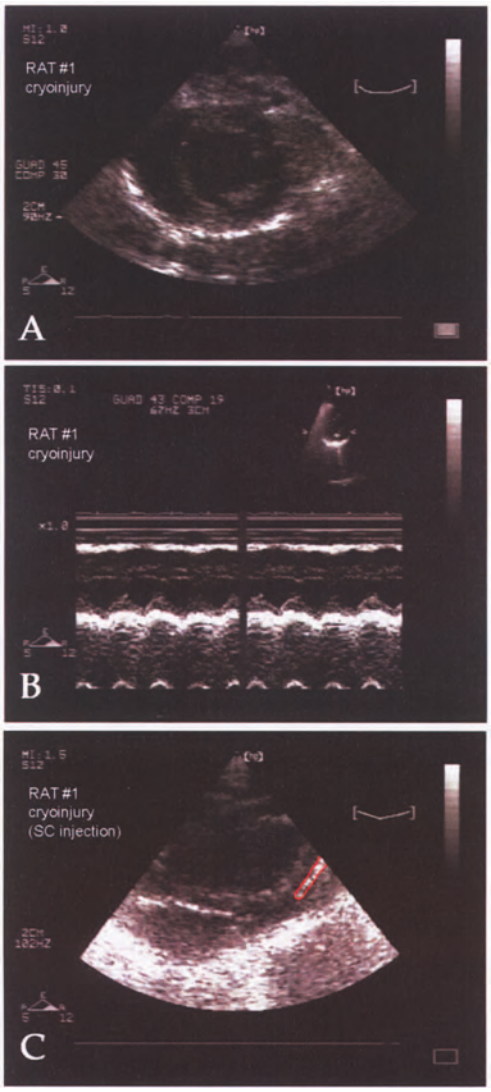

Figure 5. Echocardiographic images of a representative rat with a cryoinjured heart at day 7 after surgery, before BM-MSC transplantation (A, B). (A) Imaging of the heart in the parasternal short-axis view, in diastole. (B) M-mode echocardiogram. (C) The position of the needle (encircled with a red line) used to deliver MSCs to the left ventricle.

Cell Transplantation

Because closed-chest intramyocardial delivery of BM-MSCs or AF-MSCs in the rat heart via echocardiographic guidance can be complicated by an inadvertent injection into the LV cavity, we first practiced open-

Table 3. Distribution (in %) of Cell Proliferation and Apoptosis in Transplanted CMTMR-Labeled MSCs at Day 10 Versus Day 30 Postinjection Time

	Day 10		Day 30	
	P-Histone H3$^+$	ApopTag$^+$	P-Histone H3$^+$	ApopTag$^+$
BM-MSCs	20.95 ± 1.07*	12.37 ± 1.70†	6.79 ± 0.48*	4.68 ± 0.20†
AF-MSCs	32.75 ± 1.66*	7.40 ± 0.60†	10.83 ± 3.50*	4.16 ± 0.58†

*, †$p < 0.01$.

chest cell transplantations to ensure a correct procedure for closed-chest MSC delivery (35).

Under a general anesthesia, which reduced heart rate to 200–250 beats/min, the optimal ultrasonographic window (generally the left parasternal view) was selected in a group of cryoinjured rats (Group 2; see Table 1) kept in dorsal decubitus. A 2% solution of Evans blue dye in PBS or 10^6 GFP-labeled BM-MSCs in PBS (90 µl) was injected in the region surrounding the cryoinjury using a 30-gauge needle of an infusion set. Using 30–45° angles of injection with respect to the rat table surface, the needle was advanced through the body wall via a substernal approach. Animals injected with dye (n = 3) were sacrificed immediately whereas those injected with fluorescent cells (n = 3) were killed after 24 h. Frozen free cardiac wall was then analyzed for the histochemical and immunohistochemical distribution of dye and cellular fluorescence, respectively. In addition, cells that might have been "escaped" from the injection site or inadvertently injected in the ventricular cavity were

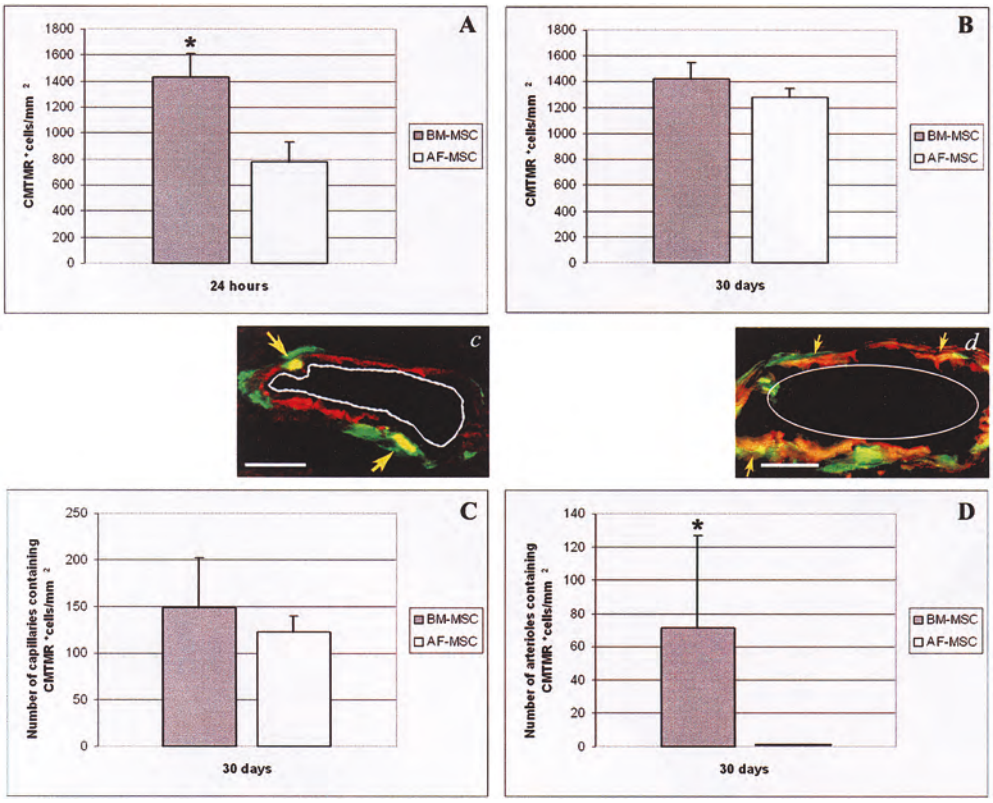

Figure 6. Comparative analysis of surviving CMTMR-positive MSCs after 24 h and 30 days in cryoinjured rat heart (A, B). Density of capillaries (C) or arterioles (D) containing a variable number of CMTMR-positive MSCs after 30 days from injection in cryoinjured heart. In (c) and (d) is shown a capillary and an arteriole, whose wall contains CMTMR$^+$ cells (yellow arrows) positive for vWf or SM α-actin, respectively, used in blood vessel counting. Scale bars: 10 µm (c); 20 µm (d).

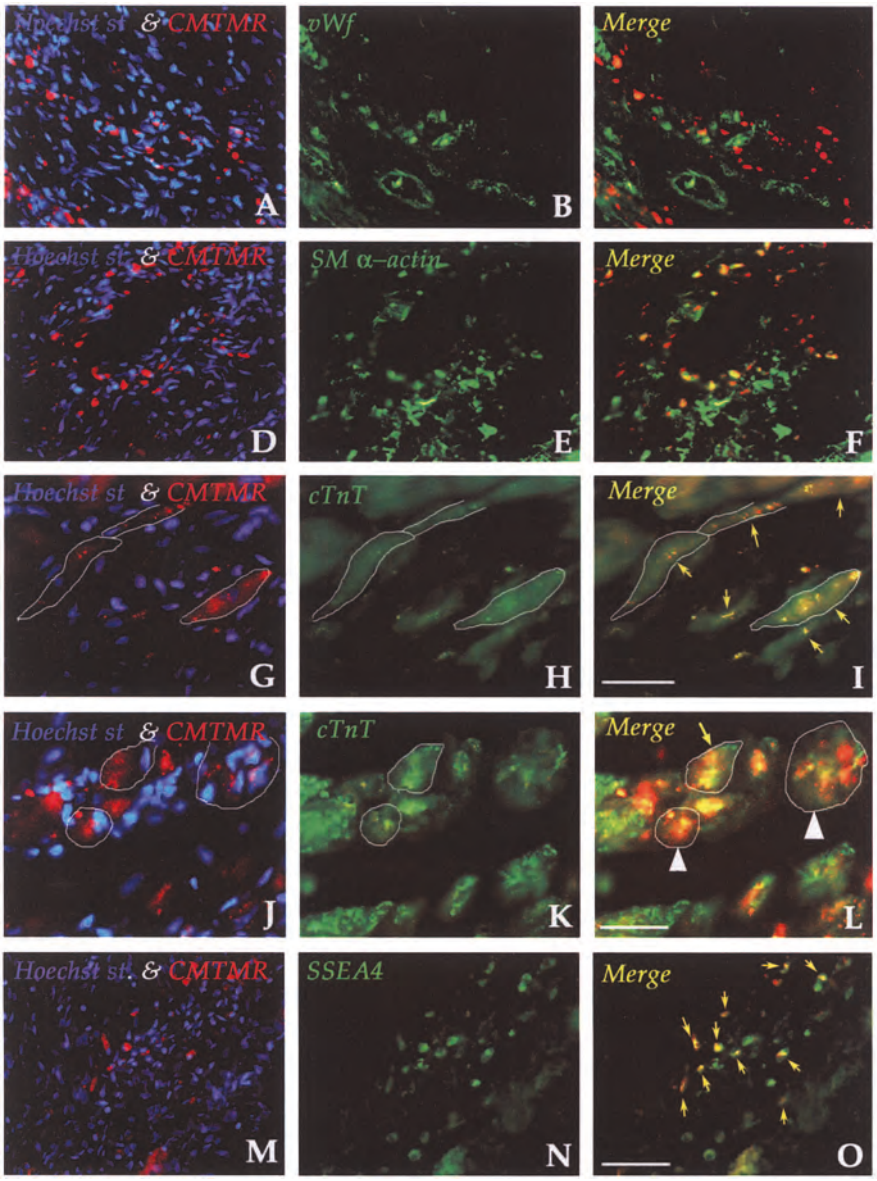

Figure 7. Immunofluorescence cell tracking of injected CMTMR-positive BM-MSCs after 30 days of transplantation tested with vWf (B), SM α-actin (E), cTnT (H, K), and SSEA4 (N). Yellow arrows indicate double-positive cells for CMTMR and the specific differentiation marker. Note that some injected cells are grouped in clusters (white arrowheads in L). Scale bars: 60 μm (A–F, M–O); 45 μm (G–I), 30 μm (J–L).

determined by examining the pulmonary parenchyma. Each lung was sectioned and 20 sections/lung analyzed by fluorescence microscopy.

Before transplantation, BM-MSCs or AF-MSCs (at the third passage) were washed extensively in MEMα and then labeled with 0.5 μM cell tracker 5-(and-6)-(4-chloromethyl(benzoyl)amino)-tetramethylrhodamine (CMTMR; Molecular Probes) according to the manufacturer's instructions. Then, cells were collected by 0.05% trypsin-EDTA treatment and viability after labeling was monitored by trypan blue exclusion test. Under the conditions used for labeling, 98% of the cells resulted positive for CMTMR and almost the same percentage (96%) resulted viable. CMTMR-labeled or GFP-expressing cells were first resuspended in MEMα without serum and then injected in rat hearts (CMTMR-MSCs, Groups 3 and 4; GFP-MSCs, Groups 5 and 6; see Table 1).

Closed-chest intramyocardial MSC transplantations

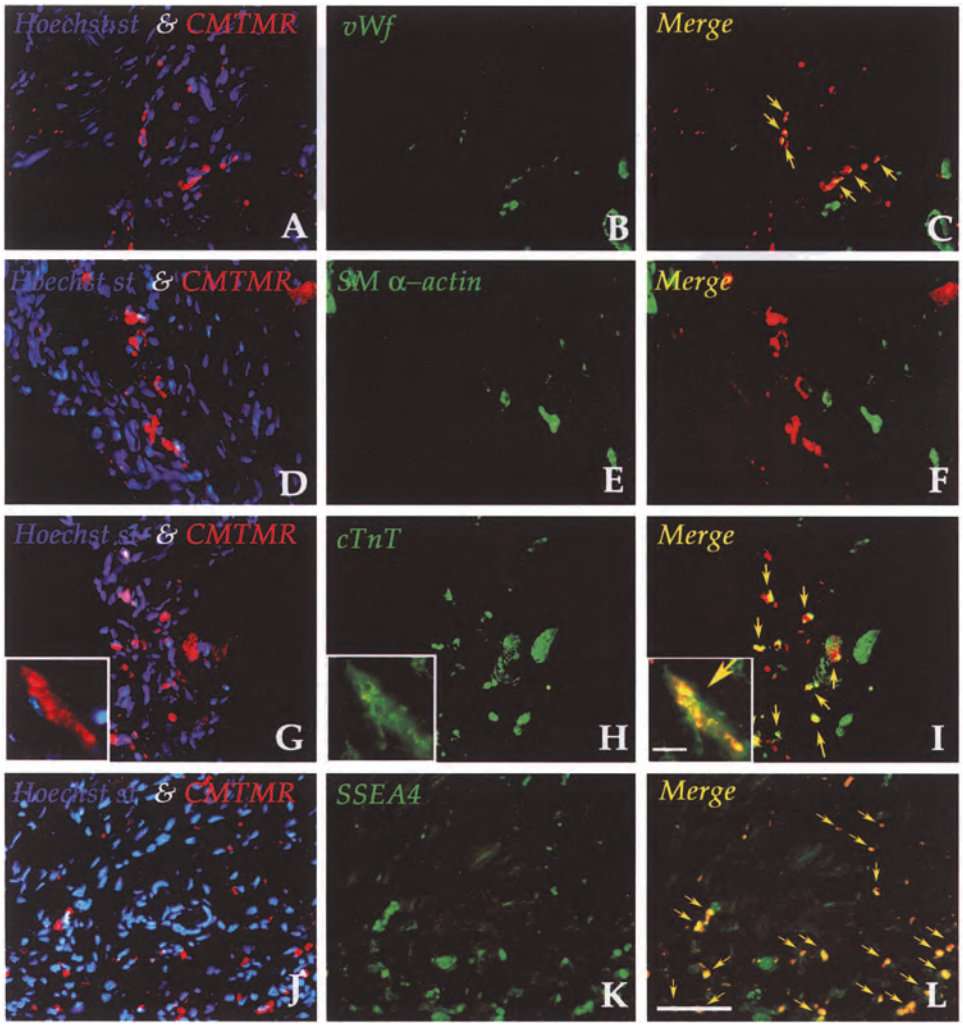

Figure 8. Immunofluorescence cell tracking of injected CMTMR-positive AF-MSCs after 30 days of transplantation tested with vWf (B), SM α-actin (E), cTnT (H), and SSEA4 (K). Yellow arrows indicate double-positive cells for CMTMR and the specific differentiation marker. A magnification of a typical cTnT-expressing CMTMR$^+$ cell is shown in insets of (G–I). Scale bars: 60 μm; insets: 45 μm.

were carried out using an oblique axis view and the needle aligned to the ventricular wall. Cell suspension (2×10^6 cells in 90 μl of solution per animal) was delivered in the periphery of the hypokinetic region (see also Figs. 4 and 5). Sham rats (Group 7, Table 1) were injected in the ANI region with the same volume of MEMα following the above-described procedure used for MSCs. Experimental animals (rats with ANI plus MEMα and rats with ANI plus CMTMR-BM-MSCs or CMTMR-AF-MSCs) were sacrificed at 1, 10, and 30 days after injections. Nude rats transplanted with GFP-BM- or AF-MSCs were sacrificed at day 30 for a comparative study. Hearts were gently rinsed in PBS, fixed in 4% *p*-formaldehyde and 30% sucrose, snap-frozen in liquid nitrogen, and stored at −80°C.

Histology, Histochemistry, and Immunohistochenistry

Analysis of inflammatory cell response that follows ANI induction was performed by histology, histochemistry, and immunohistochemistry (see also Fig. 5) on 7-μm-thick frozen cardiac sections. Extracellular matrix deposition was studied by Masson trichrome staining; angiogenesis by vWf distribution; monocyte-macrophage (Mϕ) and granulocytes (PMN) infiltration by anti-CD163 (Serotec, Oxford, UK) and anti-MCA149 (Serotec) antibodies, respectively. In addition, the following

antibodies were used to monitor the granulation tissue formation: anti-vWf (Dako), M-38 anti-procollagen I (Iowa Hybridoma Bank), anti-EIIIA fibronectin (Abcam), anti-cTnT (Abcam), and anti-SM α-actin (Sigma), anti-vimentin (Dako). HRP-conjugated anti-mouse and anti-rabbit IgGs (Dako) were used as secondary antibodies. The substrate used to reveal bound primary antibodies was 3-amino-9-ethylcarbazole (Sigma). Controls were performed using nonimmune IgGs instead of the primary antibodies or by applying the secondary antibodies alone. Antigen distribution was studied using a Leica light microscope (Leica), and images were acquired using a Leica DC300 digital videocamera (Leica). The slides were scored in a blinded fashion by two expert pathologists to determine the degree of inflammation and histological/immunohistochemical changes in cryoinjured hearts from 24 h to 30 days postinjury time.

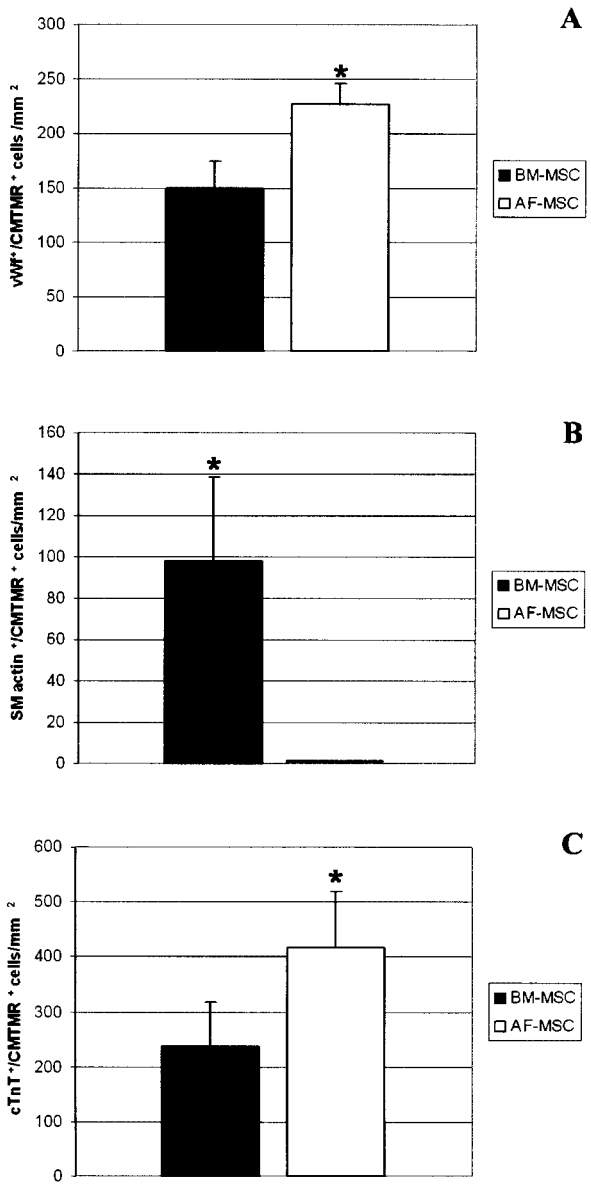

Figure 9. Density of CMTMR-positive MSCs expressing vWf (A), SM α-actin (B), or cTnT (C) 30 days after transplantation in cryoinjured heart.

Assessment of Transplanted MSC Survival, Proliferation, and Differentiation

Survival of CMTMR-labeled BM-MSCs or AF-MSCs injected in hearts of ANI rats was established 1 and 30 days after MSC transplantation using five sections per animal. Three randomly chosen microscopic fields at 100× magnification, corresponding to 0.0374 mm^2, were examined by two independent operators who counted CMTMR-positive MSCs.

Engrafted MSC proliferation and apoptosis were evaluated at 10 and 30 days from transplantation by immunofluorescence on rat heart cryosections using, respectively, an anti-phospho-Histone H3 antibody (Ser 10; Upstate, Lake Placid, NY) and the ApopTag® Plus Fluorescein In Situ Apoptosis Detection Kit (Chemicon) following the manufacturer's instructions.

Detection of differentiation marker expression in CMTMR- or GFP-transplanted BM-MSCs or AF-MSCs was performed by immunofluorescence using the antibodies to: vWf (Dako), SM α-actin (Sigma), cTnT (Abcam), *sm* (Iowa Hybridoma Bank), and SSEA4 (Chemicon). Goat anti-mouse and anti-rabbit Cy2 antibodies (Chemicon) were used as secondary antibodies. GFP-transplanted cells were identified by a rabbit anti-GFP antibody (Molecular Probes) and revealed by a Cy2-conjugated anti-rabbit secondary antibody (Chemicon). For double immunofluorescence on GFP-transplanted hearts, differentiation markers were labeled with Alexa Fluor 594-conjugated anti-mouse secondary antibody (Molecular Probes).

Differentiation of CMTMR- or GFP-labeled MSCs attained in the ANI context was studied by calculating the expression of specific markers in both organized vascular vessels (capillaries and arterioles) and nonorganized cell clusters. Capillaries were considered when stained by anti-vWf and negative for SM α-actin in serial sections. Arterioles were taken into account when parietal cells were stained by anti-SM α-actin (see also Fig. 6C and D). CM-like cells, identified by cTnT or *sm* expression, were counted both as single cell and cell clusters. Capillary density was calculated for microvessels of about 20–60 μm diameter and arteriole density was calculated for vessels of about 70–100 μm diameter. Three randomly chosen fields per section were evaluated. Only the stained vessels oriented with the lumen cut transversely were counted. The number of vessels was expressed per mm^2.

Immunofluorescence observations were carried out using a Zeiss Axioplan epifluorescence microscope and results obtained reevaluated by Leica SPS2SL confocal microscope.

Statistical Analysis

Data are expressed as the mean ± SD. Statistical differences between BM-MSCs versus AF-MSCs were determined by paired or unpaired Student *t*-tests. Results were considered statistically significant if $p < 0.01$.

RESULTS

Characterization of BM-MSCs and AF-MSCs

BM-MSCs and AF-MSCs used for cell transplantation were studied by flow cytometry and cytocentrifugation assays (Fig. 1A, Table 2). Both cell types appeared reactive for CD44, CD90, and MHCII antigens but they behaved differently for other MSC markers (i.e., CD73) (Fig. 1A). Likewise, differences in some antigen expression were also evident in cytocentrifugation assay (Table 2), especially for MSC markers CD271 and CD105, the embryonic stem cell markers SSEA4 and Oct-4, and to a lesser extent in some cell lineage-specific markers such as Flk-1 and vWf (ECs), SM22/SM α-actin (SMCs). No immunoreactivity was found for CD117 (hematopoietic stem cells) and the pan-cytokeratin antigen. Vimentin expression was similar in both MSCs.

The potential of AF-MSCs for phenotypic conversions to osteogenic, adipogenic, and cardiovascular cell lineages was evaluated in specific media and the results are shown in Figure 1B and C. AP- and Oil-Red-O-positive staining could be demonstrated after treatment with osteogenic and adipogenic inducer media, respectively (Fig. 1B). SM α-actin/SM22, which were originally weaker in AF-MSCs (Table 2), after 15 days in vitro stimulation improved their expression but to a limited extent (Fig. 1C, a, c; in both cultures the positive cells were about 15%). Conversely, vWf was present in about 50% of the respective cell populations (Fig. 1C, b, d). MSCs grown in CM-inducing media or CM-conditioned media did not show any labeling with anti-cTnT or sm antibodies (not shown). It is only with cocultures that a minority of CMFDA-labeled BM-MSCs or AF-MSCs (3.5 ± 1.0% of the respective cell population with both MSCs) also expressed the sarcomeric marker sm (Fig. 2A–F) or cTnT (not shown). Coculture experiments carried out using GFP-expressing BM-MSCs and AF-MSCs along with rat neonatal CMs (Fig. 2G–H) gave similar results (4.0 ± 1.0% of the respective cell population with both MSCs). This finding suggests that independently from genetic or nongenetic labeling the tendency of both MSCs to be converted to CM-like cells is quite low and many cells appear with more than one nucleus. We cannot say whether these cells are dividing cells or "fused" cells.

ANI Induction and MSC Transplantation

Our cryoinjury protocol applied to rat hearts was able to consistently induce an ANI that is restricted to one third to one half of the left ventricular myocardial wall (Fig. 3), the endocardial side always being spared. Thirty days from surgery only a small myocardial region still presented signs of postinjury remodeling. Echocardiographic values did not show statistically relevant changes in structural and hemodynamic parameters studied at day 7 versus day 30, suggesting that size (about 19 mm^2) and LV localization (anterior and close to the apex) of the cryolesion did not produce significant functional consequences (data not shown).

Time-related inflammatory cell infiltration, accumulation of new blood vessels, and changes in CM structure/biology and ECM matrix accumulation were monitored up to 30 days to identify the time window for cell transplantation in which the acute inflammatory response was markedly attenuated (see the Discussion section). This analysis revealed that at 7 days postinjury (Fig. 4) there were only traces of acute inflammatory cells but an abundant network of capillaries and arterioles. Hence, this time was selected for MSC transplantation and the corresponding animals injected with GFP- or CMTMR-labeled MSCs.

At this time point, MSCs were injected in the periphery of cryoinjured and control rat hearts via echocardiographic guidance (Fig. 5) and the animals sacrificed after 24 h, 10 or 30 days.

Taking into account that genetic cell tracker GFP can evoke a marked immune response (see the Discussion section), we adopted a labeling procedure based on the cellular dye CMTMR. On the other hand, we reasoned that the use of CMTMR-labeling as a tracking agent could underestimate the counting of survived transplanted cells, caused by the progressive dilution of the fluorochrome emission with cell proliferation. Preliminary data suggest that in vitro after 20 BM-MSC doublings the number of cells expressing this marker is reduced to 50% of the original staining (our unpublished data). To determine whether this also happens in our model we performed a comparative study using cryoinjured hearts from immunodeficient (rNu) rats transplanted with GFP-expressing MSCs (Groups 5 and 6, Table 1). It turned out that after 30 days from intramyocardial injections marker distribution was as follows: GFP versus CMTMR labeling was seen in 1613.18 ± 643.84 versus 1420.58 ± 129.65 cells/mm^2 (p = NS). Cardiovascular cell phenotypes were as follows: vWf^+ cells, 179.84 ± 6.33 (GFP) versus 150.36 ± 24.08 (CMTMR);

SM α-actin$^+$ cells: 88.34 ± 35.20 (GFP) versus 98.08 ± 40.84 (CMTMR); cTnT$^+$ cells: 277.01 ± 55.97 (GFP) versus 237.43 ± 79.99 (CMTMR) (p = NS). Thus, the two procedures gave slightly different results which were, however, not statistically significant.

To analyze the survival pattern of MSCs transplanted into cryoinjured hearts (Table 1, Groups 3 and 4), we first counted CMTMR-positive cells at 1 and 30 days by immunofluorescence. At 24 h after injection, BM-MSCs were more abundant than AF-MSCs (1424.50 ± 173.80 vs. 778.61 ± 156.28; $p < 0.01$), but at day 30 the number of the two MSC types was very similar (1420.58 ± 129.65 vs. 1275.26 ± 74.5; p = NS). Despite the same number of cells used in the two types of transplants, 24 h after injection the survived AF-MSCs were about one half that of BM-MSCs but with time they recovered and approached the number of BM-MSCs. This result may be compatible with a superior ability of AF-MSCs to proliferate and/or a reduced tendency to apoptosis. This issue was tackled by analyzing the distribution of phospho-Histone H3$^+$ CMTMR$^+$ MSCs in comparison to ApopTag$^+$ cells 10 and 30 days after cell transplantation in cryoinjured heart (Table 3). At day 10 AF-MSC mitotic cells were higher than BM-MSCs. At day 30 postinjection time, apoptotic cells were 4.68 ± 0.2 (BM-MSCs) versus 4.16 ± 0.58 (AF-MSCs) per mm^2 (p = NS) whereas mitotic cells were 6.79 ± 0.48 (BM-MSCs) versus 10.83 ± 1.5 (AF-MSCs) per mm^2 ($p < 0.01$). Altogether these data suggest that indeed AF-MSCs possess an in situ superior proliferative capacity, in the face of a similar apoptotic profile, and irrespective of postinjury time.

Regarding to the phenotypic potential of survived MSCs to be converted to cells expressing myocardial (cTnT$^+$ cells) and vascular (vWf$^+$ or SM α-actin$^+$ cells) antigens, only 34.6% of BM-MSCs and 49.6% of AF-MSCs were able to pursue this process. In turn, cardiovascular antigens were found expressed in cells that belong to organized microvessels (capillaries and arterioles) or dispersed in the cardiac parenchyma. About the former, 51.2% of BM-MSCs and 35.2% of AF-MSCs were found in the wall of microvessels.

Density of capillaries and arterioles containing CMTMR-positive cells (Fig. 6Cc, Dd) in this content were 148.69 ± 54.41 (BM-MSCs) and 122.49 ± 17.37 (AF-MSCs; p = NS), whereas arterioles with CMTMR-positive cells were obtained almost exclusively with BM-MSCs (71.30 ± 55.66).

Concerning single isolated cells or small cell clusters, immunofluorescence staining patterns of the two types of MSCs are shown in Figures 7 and 8. In both transplants the "embryonic stem cell" marker SSEA4 still remained expressed in the MSCs (Fig.7M–O for BM-MSCs; Fig. 8J–L for AF-MSCs). In addition, the cardiovascular cell markers cTnT, SM α-actin, and vWf were variably expressed among the injected CMTMR-positive MSCs. In particular, injected AF-MSCs seemed not be able to giving rise to SM α-actin$^+$ cells (Fig. 8A–C) and appeared mostly able to give rise to single cTnT$^+$ cells (insets in Fig. 8G–I). On the other hand, BM-MSCs appeared as single cTnT$^+$ cells (Fig. 7G–I) or clusters of positive cells (Fig. 7J–L). A comparative score of CMTMR-labeled cells positive for vWf, SM α-actin, or cTnT is shown in Figure 9. vWf-positive cells were 150.36 ± 24.08 with BM-MSCs and 227.27 ± 18.91 with AF-MSCs ($p < 0.01$). SM α-actin-positive cells were 98.03 ± 40.84 with BM-MSCs whereas almost no positive cells were found with AF-MSCs. Interestingly, these last cells were, however, able to gave a marked expression with cTnT (i.e., 417.91 ± 100.95), which was higher than BM-MSCs (237.43 ± 79.99; $p < 0.01$).

DISCUSSION

The major finding reported in this study is that fetal- or adult-type MSCs derived from AF or BM, despite a similar biological profile, do not possess an equal differentiation potential when examined in a nontransmural model of myocardial injury.

While the notion of MSCs in BM is well established, that of MSCs in AF is less common, although it has recently demonstrated that these cells are found in humans (7,17,20,39) and studied in a model of bladder cryoinjury in rats (8). Rat AF-MSCs in their "undifferentiated state" (i.e., when cultivated in the absence of specific differentiation conditions) share a common antigenic profile with rat BM-MSCs as well as the human counterpart (7,17,20,39) and MSCs from other human tissues (31). Rat AF-MSCs express CD44, CD73, CD90, CD105, CD271, and vimentin but are negative no for CD45, CD117, MHCII, or the pan-cytokeratin antigen. In addition, rat AF-MSCs can be induced to osteogenic and adipogenic cell lineages in vitro, which make these cells similar to BM-MSCs (27). A similar behavior has recently been reported for amnion-derived MSCs isolated from embryonic day 18.5 rat fetuses (27). We cannot exclude that part of rat MSCs from the AF described here can indeed derive from the amnion as may also occur in humans (7,28).

Some phenotypic features are, however, distinct in rat AF-MSCs (e.g., lower expression of the stromal-associated cell marker CD73 and higher expression of the "embryonic stem cell" markers Oct-4 and SSEA4) (Table 2). BM-MSCs seem inherently more "disposed" to a myofibroblast phenotype (a higher proportion of SM α-actin and SM22, markers of SMC lineage). Unique functional features, colony formation capacity, cell proliferation, and gene expression profile have been described in MSCs from different tissue sources (38,

43,48). More recently, transcriptome analysis of human AF and BM has confirmed that MSCs display both a specific gene profile and a common "gene core" involved in the regulation of extracellular matrix and adhesion and signaling (38).

When in vitro differentiation of MSCs is "pushed" by culturing these cells in the presence of EC- or SMC-inducing media or neonatal CM, both MSCs respond to the changes in the microenvironment by improving their propensity for vascular cell differentiation and only slightly for the CM cell lineage. The role played by cell–cell contact or soluble factors in inducing BM-MSC-to-CM phenotype conversion is controversial (4, 25,45). In our hands, both MSCs seem to require mostly a physical interaction to achieve expression of a sarcomeric markers, but this is probably a first step in the differentiation–maturation pathway and does not necessarily imply that a complete phenotypic maturation has been achieved (e.g., the SSEA4 marker is still expressed, data not shown). This behavior is shared with other stem cell populations such as the c-kit$^+$ multilineage, cardiogenic stem cells that display in vitro an incomplete morphological and functional pattern (12). We cannot rule out that the apparent CM-like phenotype shown in vitro (Fig. 2) or in vivo (Figs. 7 and 8) is due to fusion of MSCs with CMs as an alternative to transdifferentiation (12).

The differentiation potentials of MSCs observed in vitro need a definitive in vivo confirmation for future cell therapy experiments/trials aimed at replenishing damaged cardiovascular tissue. As a first step in this bench-to-bed pathway we set up a cryoinjury model that generates a restricted epicardial-myocardial lesion. It was not our intention to ascertain if MSC transplantation is able to reverse a potential cardiac dysfunction, possibly caused by the cryolesion (6,26). We have simply chosen the cryoinjury model and syngeneic rats to study the phenotypic potential of these two types of MSCs because in our experience this procedure gives a well-delimited and reproducible damage (8), low or no mortality, and a necrotic inflammatory healing process that can be reminiscent of the one found in the ischemic injury (see, e.g., Fig. 4) (6). With this procedure, which entails a small cryoprobe, a limited number of applications of the cryoprobe on the epicardial surface, a peculiar anatomical localization of injury, we induced a nontrasmural lesion with no echocardiographic evidence for functional changes or a significant structural remodeling.

One important advantage of the ANI model is that it allows for a precise identification of reproducible postinjury spatiotemporal changes (inflammatory cell infiltration, in particular) and the localization of the border zone between the necrotic area and surrounding tissue (which includes the reactive granulation tissue) to inject MSCs. In addition, with this model it becomes possible to select precisely the "time window" that is thought to be appropriate for MSC delivery. In this regard, the postinjury administration of cells to be injected intramyocardially is tackled in two different ways: some authors postulate that stem cells can attain a better homing, survival, engraftment, and differentiation if administrated soon after injury whereas others point to the presumed role of cytokines, chemokines, and loss of surviving factors in causing death of grafted cells (10,13,18). Another potential effect of time-dependent delivery of MSCs in the injured heart relies on the capacity to exert an efficacious paracrine role on the surrounding, reversible damaged CMs. This aspect has not been taken into account and it will be targeted in future studies. Ongoing studies confirm that when AF-MSCs and BM-MSCs are injected at the time of ANI the cell survival at day 30 postinjury is about one half of that obtained with injections made 7 days after injury (unpublished data). In addition, the targeted delivery of MSCs to the tissue surrounding the organizing ANI region carried out by echocardiographic guidance may allow a better survival and a higher MSC commitment for cardiovascular cell conversion (18). In fact, MSCs can take advantage of the peculiar environment, almost devoid of inflammatory cells (see Fig. 4) at the time of intramyocardial transplantation, but still containing cytokines and growth factors (such as VEGF) useful for MSC-mediated cardiovascular cell repair (46).

We have, on purpose, selected to use the cell tracker CMTMR instead of the "classic" genetic marker GFP to monitor the in vivo phenotypic potential of MSCs. Injection of MSCs in immunocompetent ANI rats is potentially able to evoke a humoral and cellular immune response in the time period of 30 days, thus contributing to cell graft rejection (29,36). Once transplanted in the cryoinjured rat hearts the two types of MSCs do not show any graft rejection but reveal a different survival pattern and cardiovascular cell potential. AF-MSCs after 24 h from injection are less numerous than BM-MSCs but this difference becomes less evident after 30 days, suggesting that the initial loss of AF-MSCs in the new cardiac environment can be recovered by cell proliferation and/or long-term resistance to cell apoptosis. In fact, while a paracrine antiapoptotic effect of BM-MSCs on CMs surrounding the damaged myocardial region is known (40), nothing is acknowledged about a possible autocrine action of released factors from BM-MSCs or AF-MSCs. More importantly, while the two MSCs can contribute roughly at the same extent to capillary formation, AF-MSCs are not able to participate in the formation of arterioles and hence to vascular SMCs. This behavior is also confirmed by the absence of AF-MSCs expressing SM α-actin not only in the forming arterioles but also in CMTMR-positive dispersed cells. On the

other hand, AF-MSCs display an inherent higher propensity for expressing the EC marker vWf and the CM marker cTnT. The in vivo pattern observed with transplanted MSCs is mirrored by the in vitro profile (i.e., BM-MSCs seem to be inherently more inclined to form myofibroblasts). It is known that MSCs are present in several adult organs/tissues (31), but this does not imply that they have equal differentiation potentials. For example, synovium-derived MSCs and BM-MSCs show a similar ability to suppress T-cell response in a mixed lymphocyte reaction but different transcriptional profiles and osteogenic capacities (9). Clearly, the existence of a peculiar differentiation potential in a given MSC population is likely to be relevant when the MSCs are transplanted in a new "niche" (e.g., in the heart) or are derived from donors of different ages. In general, fetal MSCs have higher proliferative capacity and are less lineage committed than adult MSCs (22,44).

We cannot say what makes AF-MSCs less suitable for a complete vascular recovery in this ANI model, but it is clear from our previous studies that these cells, when transplanted in a porcine model of myocardial ischemia, can be converted to vascular cells but not to cardiomyocytes (32). This suggests a species-specific or microenvironment-dependent (myocardial cryoinjury, rat vs. coronary artery thrombosis, pig) differentiation potential. On this ground, the differential ability of MSCs to form new cardiovascular cells/tissue must be carefully taken into account if they are to be used in a context of human cell therapy of myocardial ischemia. Certainly, the scarce capacity of AF-MSCs, as such, to form arterioles may hamper their application in cardiopathic patients that cannot rely solely on neoangiogenesis for blood perfusion of damaged heart (44).

ACKNOWLEDGMENTS: This work was supported in part by grants from Biomedical Association for Vascular Research and Consortium Agreement European Community "Heart failure and cardiac repair," IP 018630. P. De Coppi was supported by Citta'della Speranza, Onlus.

REFERENCES

1. Anversa, P.; Kajstura, J.; Leri, A.; Bolli, R. Life and death of cardiac stem cells. Circulation 113:1451–1463; 2006.
2. Baksh, D.; Yao, R.; Tuan, R. S. Comparison of proliferative and multilineage differentiation potential of human mesenchymal stem cells derived from umbilical cord and bone marrow. Stem Cells 25:1384–1392; 2007.
3. Barry, F. P.; Murphy, J. M.; English, K.; Mahon, B. P. Immunogenicity of adult mesenchymal stem cells: Lessons from the fetal allograft. Stem Cells Dev. 14:252–265; 2005.
4. Beltrami, A. P.; Barlucchi, L.; Torella, D.; Baker, M.; Limana, F.; Chimenti, S.; Kasahara, H.; Rota, M.; Musso, E.; Urbanek, K.; Leri, A.; Kajstura, J.; Nadal-Ginard, B.; Anversa, P. Adult cardiac stem cells are multipotent and support myocardial regeneration. Cell 114:763–776; 2003.
5. Boheler, K. R.; Czyz, J.; Tweedie, D.; Yang, H. T.; Anisimov, S. V.; Wobus, A. M. Differentiation of pluripotent embryonic stem cells into cardiomyocytes. Circ. Res. 91: 189–201; 2002.
6. Ciulla, M. M.; Paliotti, R.; Ferrero, S.; Braidotti, P.; Esposito, A.; Gianelli, U.; Busca, G.; Cioffi, U.; Bulfamante, G.; Magrini, F. Left ventricular remodeling after experimental myocardial cryoinjury in rats. J. Surg. Res. 116:91–97; 2004.
7. De Coppi, P.; Bartsch, Jr., G.; Siddiqui, M. M.; Xu, T.; Santos, C. C.; Perin, L.; Mostoslavsky, G.; Serre, A. C.; Snyder, E. Y.; Yoo, J. J.; Furth, M. E.; Soker, S.; Atala, A. Isolation of amniotic stem cell lines with potential for therapy. Nat. Biotech. 25:100–106; 2007.
8. De Coppi, P.; Callegari, A.; Chiavegato, A.; Gasparotto, L.; Piccoli, M.; Taiani, J.; Piccoli, M.; Lenzini, E.; Gerosa, G.; Vendramin, I.; Cozzi, E.; Angelini, A.; Iop, L.; Zanon, G. F.; Atala, A.; De Coppi, P.; Sartore, S. Amniotic fluid and bone marrow derived mesenchymal stem cells can be converted to smooth muscle cells in the cryo-injured rat bladder and prevent compensatory hypertrophy of surviving smooth muscle cells. J. Urol. 177:369–376; 2007.
9. Djouad, F.; Bony, C.; Haupl, T.; Uze, G.; Lahlou, N.; Louis-Plence, P.; Apparailly, F.; Canovas, F.; Rème, T.; Sany, J.; Jorgensen, C.; Noël, D. Transcriptional profiles discriminate bone marrow-derived and synovium-derived mesenchymal stem cells. Arthritis Res. Ther. 7:R1304–1315; 2005.
10. Ebelt, H.; Jungblut, M.; Zhang, Y.; Kubin, T.; Kostin, S.; Technau, A.; Oustanina, S.; Niebrügge, S.; Lehmann, J.; Werdan, K.; Braun, T. Cellular cardiomyoplasty: Improvement of left ventricular function correlates with the release of cardioactive cytokines. Stem Cells 25:236–244; 2007.
11. Ertl, G.; Frantz, S. Healing after myocardial infarction. Cardiovasc. Res. 66:22–32; 2005.
12. Garbade, J.; Schunert, A.; Rastan, A. J.; Lenz, D.; Walther, T.; Gummert, J. F.; Dhein, S.; Mohr, F. W. Fusion of bone marrow-derived stem cells with cardiomyocytes in a heterologous *in vitro* model. Eur. J. Cardiothorac. Surg. 28:685–691; 2005.
13. Guo, J.; Lin, G. S.; Bao, C. Y.; Hu, Z. M.; Hu, M. Y. Anti-inflammation role for mesenchymal stem cells transplantation in myocardial infarction. Inflammation 30:97–104; 2007.
14. Harty, M.; Neff, A. W.; King, M.; Mescher, A. L. Regeneration or scarring: An immunological perspective. Dev. Dyn. 226:268–279; 2003.
15. Heil, M.; Schaper, W. Influence of mechanical, cellular, and molecular factors on collateral artery growth (arteriogenesis). Circ. Res. 95:449–458; 2004.
16. Henning, R. J.; Burgos, J. D.; Ondrovic, L.; Sanberg, P.; Balis, J.; Morgan, M. B. Human umbilical cord blood progenitor cells are attracted to infarcted myocardium and significantly reduce myocardial infarction size. Cell Transplant. 15:647–658; 2006.
17. in't Anker, P. S.; Scherjon, S. A.; Kleijburg-van der Keur, C.; Noort, W. A.; Claas, F. H.; Willemze, R.; Fibbe, W. E.; Kanhai, H. H. Amniotic fluid as a novel source of mesenchymal stem cells for therapeutic transplantation. Blood 102:1548–1549; 2003.
18. Jaquet, K.; Krause, K. T.; Denschel, J.; Faessler, P.; Nauerz, M.; Geidel, S.; Boczor, S.; Lange, C.; Stute, N.; Zander, A.; Kuck, K. H. Reduction of myocardial scar size after implantation of mesenchymal stem cells in rats: What is the mechanism? Stem Cells Dev. 14:299–309; 2005.
19. Khurana, R.; Simons, M.; Martin, J. F.; Zachary, I. C. Role of angiogenesis in cardiovascular disease: A critical appraisal. Circulation 112:1813–1824; 2005.

20. Kim, J.; Lee, Y.; Kim, H.; Hwang, K. J.; Kwon, H. C.; Kim, S. K.; Cho, D. J.; Kang, S. G.; You, J. Human amniotic fluid-derived stem cells have characteristics of multipotent stem cells. Cell Prolif. 40:75–90; 2007.
21. Landmesser, U.; Drexler, H. Chronic heart failure: An overview of conventional treatment versus novel approach. Nat. Clin. Pract. Cardiovasc. Med. 2:628–638; 2005.
22. Lee, C. C.; Ye, F.; Tarantal, A. F. Comparison of growth and differentiation of fetal and adult rhesus monkey mesenchymal stem cells. Stem Cells Dev. 15:209–220; 2006.
23. Leri, A.; Kajstura, J.; Anversa, P. Cardiac stem cells and mechanisms of myocardial regeneration. Physiol. Rev. 85: 1373–1416; 2005.
24. Li, C. D.; Zhang, W. Y.; Li, H. L.; Jiang, X. X.; Zhang, Y.; Tang, P.; Mao, N. Mesenchymal stem cells derived from human placenta suppress allogeneic umbilical cord blood lymphocyte proliferation. Cell Res. 15:539–547; 2005.
25. Li, X.; Yu, X.; Lin, Q.; Deng, C.; Shan, Z.; Yang, M.; Lin, S. Bone marrow mesenchymal stem cells differentiate into functional cardiac phenotypes by cardiac microenvironment. J. Mol. Cell. Cardiol. 42:295–303; 2007.
26. Marchlinski, F. E.; Falcone, R.; Iozzo, R. V.; Reichek, N.; Vassallo, J. A.; Eysmann, S. B. Experimental myocardial cryoinjury: Local electromechanical changes, arrhythmogenicity, and methods for determining depth of injury. PACE 10:886–901; 1987.
27. Marcus, A. J.; Coyne, T. M.; Rauch, J.; Woodbury, D.; Black, I. B. Isolation, characterization, and differentiation of stem cells derived from rat amniotic membrane. Differentiation 76:130–144; 2008.
28. Miki, T.; Lehman, T.; Cai, H.; Stolz, D. B.; Strom, S. C. Stem cell characteristics of amniotic epithelial cells. Stem Cells 23:1549–1559; 2005.
29. Morris, J. C.; Conerly, M.; Thomasson, B.; Storek, J.; Riddell, S. R.; Kiem, H. P. Induction of cytotoxic T-lymphocyte response to enhanced green and yellow fluorescent proteins after myeloablative conditioning. Blood 103:492–499; 2004.
30. Nishiyama, N.; Miyoshi, S.; Hida, N.; Uyama, T.; Okamoto, K.; Ikegami, Y.; Miyado, K.; Segawa, K.; Terai, M.; Sakamoto, M.; Ogawa, S.; Umezawa, A. The significant cardiomyogenic potential of human umbilical cord blood-derived mesenchymal stem cells *in vitro*. Stem Cells 25(8):2017–2024; 2007.
31. Pittenger, M. F.; Martin, B. J. Mesenchymal stem cells and their potential as cardiac therapeutics. Circ. Res. 95: 9–20; 2004.
32. Sartore, S.; Lenzi, M.; Angelini, A.; Chiavegato, A.; Gasparotto, L.; De Coppi, P.; Bianco, R.; Gerosa, G. Amniotic mesenchymal cells autotransplanted in a porcine model of cardiac ischemia do not differentiate to cardiogenic phenotypes. Eur. J. Cardiothorac. Surg. 28:677–684; 2005.
33. Shim, W. S.; Jiang, S.; Wong, P.; Tan, J.; Chua, Y. L.; Tan, Y. S.; Sin, Y. K.; Lim, C. H.; Chua, T.; Teh, M.; Liu, T. C.; Sim, E. Ex vivo differentiation of human adult bone marrow stem cells into cardiomyocyte-like cells. Biochem. Biophys. Res. Commun. 324:481–488; 2004.
34. Sjaastad, I.; Sejersted, O. M.; Ilebekk, A.; Bjørnerheim, R. Echocardiographic criteria for detection of postinfarction congestive heart failure in rats. J. Appl. Physiol. 289: 1445–1454; 2000.
35. Springer, M. L.; Sievers, R. E.; Viswanathan, M. N.; Yee, M. S.; Foster, E.; Grossman, W.; Yeghiazarians, Y. Closed-chest cell injections into mouse myocardium guided by high-resolution echocardiography. Am. J. Physiol. Heart Circ. Physiol. 289:H1307–H1314; 2005.
36. Stripecke, R.; del Carmen Villacres, M.; Skelton, D. C.; Satake, N.; Halene, S.; Kohn, D. B. Immune response to green fluorescent protein: implications for gene therapy. Gene Ther. 6:1305–1312; 1999.
37. Swijnenburg, R. J.; Tanaka, M.; Vogel, H.; Baker, J.; Kofidis, T.; Gunawan, F.; Lebl, D. R.; Caffarelli, A. D.; de Bruin, J. L.; Fedoseyeva, E. V.; Robbins, R. C. Embryonic stem cell immunogenicity increases upon differentiation after transplantation into ischemic myocardium. Circulation 112(9 Suppl.):I166–172; 2005.
38. Tsai, M. S.; Hwang, S. M.; Chen, K. D.; Lee, Y. S.; Hsu, L. W.; Chang, Y. J.; Wang, C. N.; Peng, H. H.; Chang, Y. L.; Chao, A. S.; Chang, S. D.; Lee, K. D.; Wang, T. H.; Wang, H. S.; Soong, Y. K. Functional network analysis on the transcriptomes of mesenchymal stem cells derived from amniotic fluid, amniotic membrane, cord blood, and bone marrow. Stem Cells 25(10):2511–2523; 2007.
39. Tsai, M. S.; Lee, J. L.; Chang, Y. J.; Hwang, S. M. Isolation of human multipotent mesenchymal stem cells from second-trimester amniotic fluid using a novel two-stage culture protocol. Hum. Reprod. 19:1450–1456; 2005.
40. Uemura, R.; Xu, M.; Ahmad, N.; Ashraf, M. Bone marrow stem cells prevent left ventricular remodeling of ischemic heart through paracrine signalling. Circ. Res. 98: 1414–1421; 2006.
41. Vaananen, H. K. Mesenchymal stem cells. Ann. Med. 37: 469–479; 2005.
42. Vats, A.; Bielby, R. C.; Tolley, N. S.; Nerem, R.; Polak, J. M. Stem cells. Lancet 366:592–602; 2005.
43. Wagner, W.; Wein, F.; Seckinger, A.; Frankhauser, M.; Wirkner, U.; Krause, U.; Blake, J.; Schwager, C.; Eckstein, V.; Ansorge, W.; Ho, A. D. Comparative characteristics of mesenchymal stem cells from human bone marrow, adipose tissue, and unbilical cord blood. Exp. Hematol. 33:1402–1416; 2005.
44. Wollert, K. C.; Drexler, H. Cell-based therapy for heart failure. Curr. Opin. Cardiol. 21:234–239; 2006.
45. Xu, M. F.; Wani, M.; Dai, Y. S.; Wang, J.; Yan, M.; Ayub, A.; Ashraf, M. Differentiation of bone marrow stromal cells into the cardiac phenotype required intercellular communication with myocytes. Circulation 110:2658–2665; 2004.
46. Yau, T. M.; Li, G.; Weisel, R. D.; Reheman, A.; Jia, Z. Q.; Mickle, D. A.; Li, R. K. Vascular endothelial growth factor transgene expression in cell-transplanted hearts. J. Thorac. Cardiovasc. Surg. 127:1180–1187; 2004.
47. Yen, B. L.; Huang, H. I.; Chien, C. C.; Jui, H. Y.; Ko, B. S.; Yao, M.; Shun, C. T.; Yen, M. L.; Lee, M. C.; Chen, Y. C. Isolation of multipotent cells from human term placenta. Stem Cells 23:3–9; 2005.
48. Yoshimura, H.; Muneta, T.; Rimura, A.; Yokoyama, A.; Koga, H.; Sekiya, I. Comparison of rat mesenchymal stem cells derived from bone marrow, synovium, periosteum, adipose tissue, and muscle. Cell Tissue Res. 327:449–462; 2007.
49. Zhang, Y. M.; Hartzell, C.; Narlow, M.; Dudley, Jr., S. C. Stem cell-derived cardiomyocytes demonstrate arrhythmic potential. Circulation 106:1294–1299; 2002.
50. Zuk, P. A.; Zhu, M.; Ashjian, P.; De Ugarte, D. A.; Huang, J. I.; Mizuno, H.; Alfonso, Z. C.; Fraser, J. K.; Benhaim, P.; Hedrick, M. H. Human adipose tissue is a source of multipotent stem cells. Mol. Biol. Cell 13:4279–4295; 2002.